

# Photocurrent analysis of $\text{AgIn}_5\text{S}_8$ crystal

MAHMUT BUCURGAT<sup>1,\*</sup>, SELAHATTIN OZDEMIR<sup>2</sup> and TEZER FIRAT<sup>3</sup>

<sup>1</sup>Department of Physics, Faculty of Science, Gazi University, 06500 Ankara, Turkey

<sup>2</sup>Department of Physics, Faculty of Arts and Sciences, Middle East Technical University, 06531 Ankara, Turkey

<sup>3</sup>Department of Physics Engineering, Hacettepe University, 06800 Ankara, Turkey

MS received 6 October 2015; accepted 15 April 2016

**Abstract.** The photocurrent (PC) spectrum of  $\text{AgIn}_5\text{S}_8$  crystal consists of a single peak, which provides to determine the bandgap energy by applying the Moss rule. The temperature dependence of the bandgap energy was also calculated. The PC dramatically increased by pre-illumination with light having wavelength corresponding to the bandgap of  $\text{AgIn}_5\text{S}_8$ . The temperature-dependent PC of the sample was measured at different temperatures from 80 to 300 K and the PC spectrum consisted a single broad peak. Thermal quenching of the PC was observed to start at  $\sim 105$  K and the PC completely quenched at  $\sim 180$  K. The quenching mechanism was discussed in terms of the two-centre model. The height of the PC peak risen linearly with applied voltage up to 5.0 V under constant intensity of light. Similarly, the dark current–voltage characteristics consisted of a single region dominating an ohmic behaviour, and no space charge limited region was apparent at various temperatures up to 20 V.

**Keywords.** Photocurrent; spectral distribution; trapping; temperature dependence; thermal quenching.

## 1. Introduction

$\text{AgIn}_5\text{S}_8$  crystals have been studied for a long time, as they have a high sensitivity to light [1,2] in the visible region with unique optical properties [3–12]. Earlier studies have reported indirect bandgap of this crystal as 1.8 and 1.9 eV at 300 and 96 K, respectively [1].  $\text{AgIn}_5\text{S}_8$  crystal may be one of the good semiconductor candidate for photovoltaic solar cell applications [13–16].

Impurities and/or oxygen in many crystals play important role in their electrical and photoelectrical properties. The long-term stability is also one of the major problems of this type of materials. Primarily, oxygen acts as an acceptor in sulphur-containing compound semiconductors like CdS and PbS [17]. Woods [18] has found that CdS crystals showed a decrease in photosensitivity under strong exposure to oxygen and the destroying photosensitivity was attributed to the diffusion of oxygen into sulphur vacancies. To our knowledge till date, there is only one published work [19] in the literature on the application of solar cells by using  $\text{AgIn}_5\text{S}_8$  crystals. Even in this work there is no information about the sustained stability of  $\text{AgIn}_5\text{S}_8$ . Although we have not measured the stability, we believe that  $\text{AgIn}_5\text{S}_8$  may not be the exception and our sample should also be effected by oxygen diffusion to the sulphur vacancies during the long-term use.

The electrical and optical characteristics of the semiconductors are strongly affected by the electron and/or hole trapping states causing some complications in the interpretation of the results. Thus, it is important to obtain some information about the effect of the traps on the photocurrent (PC).

The analysing of the PC is usually complicated because the shape, distribution and the magnitude of the PC are strongly influenced by the amount of filling of the traps during or prior to the measurement. The light intensity, exposure due to previous measurement and the pre-illumination time are investigated. Besides, the dark background current, both temperature and spectral dependencies of the PC of  $\text{AgIn}_5\text{S}_8$  crystal are presented here. However, in the literature, only a spectral distribution of PC for  $\text{AgIn}_5\text{S}_8$  crystal is reported by Akihiro *et al* [1]. In this study, the spectral and the temperature-dependent PC for unintentionally doped  $\text{AgIn}_5\text{S}_8$  crystal is systematically investigated. The work focuses on both the effect of pre-illumination and successive measurement of the PC from the wavelength 450 to 730 nm. The traps are filled by the bandgap light (659 nm), which is just high enough for generation of electron–hole pairs in this crystal. We previously determined the characteristics of traps in the  $\text{AgIn}_5\text{S}_8$  crystal [20] and we utilized the sample from the same batch in this investigation.

In this study, we observed for the first time that the temperature-dependent PC of  $\text{AgIn}_5\text{S}_8$  crystal exhibits a thermal quenching. It is hoped that this study will give some unique information on the charge carriers transport influenced by the traps in the  $\text{AgIn}_5\text{S}_8$  crystal. In spite of its very high sensitivity to light,  $\text{AgIn}_5\text{S}_8$  crystal has not been studied for some details yet. A few articles [6,16] in the literature focused on the photoelectrical properties of  $\text{AgIn}_5\text{S}_8$  crystals. However, PC measurements [1] are only limited to a spectral distribution in liquid nitrogen and room temperatures. The present study investigates the PC in  $\text{AgIn}_5\text{S}_8$  crystal in a wide temperature range between 80 and 300 K. This work also presents both the chemical composition of our  $\text{AgIn}_5\text{S}_8$

\*Author for correspondence (mahmut.bucurgat@gazi.edu.tr)

sample determined from the energy dispersive X-ray analysis (EDXA) and the structural characterization made by the X-ray diffraction (XRD) spectroscopy.

## 2. Experiment

AgIn<sub>5</sub>S<sub>8</sub> crystal used in this investigation is grown by modified Bridgeman method with high resistivity ( $\sim 10^6$  ohm cm<sup>-1</sup> at room temperature). The resistivity of the sample is determined from the current–voltage measurements in dark. The sample is cleaved perpendicular to the crystal axis with a dimension of  $5 \times 6 \times 1$  mm<sup>3</sup>. The semiconductor sample is determined as n-type by the use of the hot probe method. Thermally evaporated silver with purity 99.99% is used to form the contacts on both sides with a 100 nm thickness. A window area of  $\sim 9$  mm<sup>2</sup> is formed on the electrode of the front face to provide illumination to the surface and thin silver wires are indium soldered to the electrodes. The sample is heat treated at 320 K for 10 min in the cryostat at a low pressure of  $\sim 1 \times 10^{-5}$  torr provided by the turbomolecular pump (Pfeiffer Hi Cube) in order to empty all the traps.

All measurements of the dark current, temperature-dependent PC and thermally stimulated current (TSC) are carried out at slow heating rates under low voltages from 80 to 300 K by using a Keithley 6514 electrometer. A Si diode with an accuracy of  $\pm 0.1$  K was utilized to make the measurement and to control the temperature in the cryostat (JANIS VPF-475) through a Lakeshore-321 temperature controller. The experimental data were collected and stored in a personal computer during the measurements. The traps are filled by a monochromatic light with photon energy  $\sim 1.9$  eV obtained by an interference filter before each run of the TSC measurements. The PC spectral distribution measurements

were performed between the wavelengths of 450 and 730 nm for a period of 20 min with the wavelength accuracy of  $\sim 3.0$  nm. Ealing 5180 monochromator coupled with 150 W Tungsten-Halogen lamp (Motic MLC-150C) was used for the PC excitation. The PC spectra are normalized for constant number of photons cm<sup>-2</sup> s<sup>-1</sup> for each wavelength. The majority of the measurements were performed under a low electric field of 1 V cm<sup>-1</sup>; thus, the possibility of field emission from traps would be disregarded. Both TSC and the PC are measured at a low heating rate of 2 K min<sup>-1</sup> to minimize the thermal gradient between the bottom and the top of the sample.

## 3. Results and discussion

### 3.1 Crystal structure and chemical composition

The crystal structure of our AgIn<sub>5</sub>S<sub>8</sub> sample in the form of powder was analysed by using XRD system (Rigaku Ultima-IV with CuK $\alpha$  radiation ( $\lambda = 0.154$  nm)). The diffractogram was obtained at a low speed (1.0 deg min<sup>-1</sup>) with voltage of 40 kV in the  $2\theta$  diffraction angle from 10 to 70° (figure 1).

The XRD result of our AgIn<sub>5</sub>S<sub>8</sub> sample was matched to cubic spinel standard space group Fd-3m (227). All the measured peaks are best matched to a pure cubic phase by International Center for Diffraction Data (ICDD) card number 01-070-5631 and the Miller indices (hkl) of the structure are shown in figure 1. The lattice parameter of the unit cell is 10.8265 Å. The sharp diffraction peaks approve the well crystallinity and purity of the phases of our sample. Furthermore, it may be emphasized from figure 1 that the highest intensity of (311) peak is well in accordance with the ICDD card. Besides, the intensity of (400) peak (45%) is

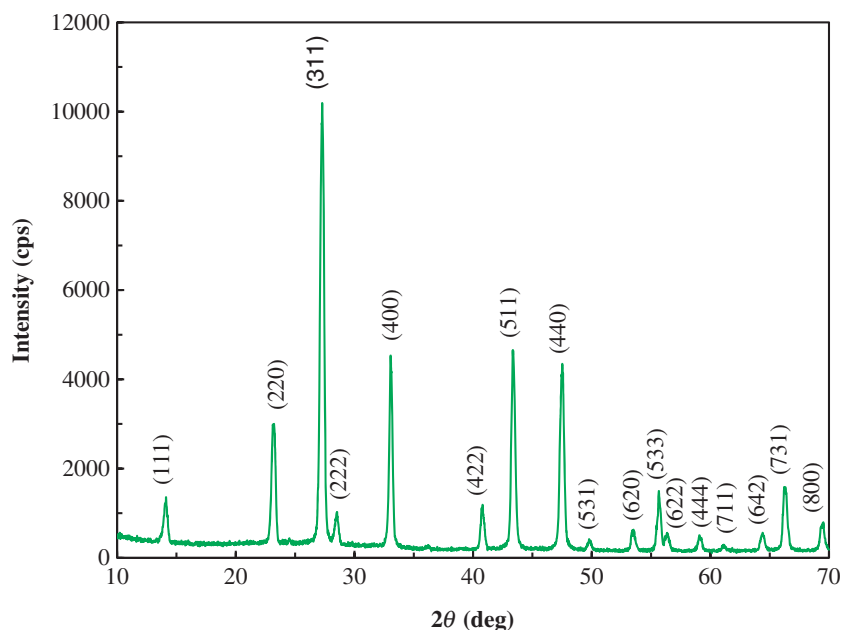


**Figure 1.** The X-ray powder diffraction pattern of AgIn<sub>5</sub>S<sub>8</sub> sample.

much higher than that of the ICDD card (24%). Meanwhile, intensities of other peaks are well in accordance with those of the ICDD card.

In addition, the elemental composition of our  $\text{AgIn}_5\text{S}_8$  sample was found by the use of EDXA. The EDXA is a technique used to identify the elemental composition of materials. In this technique, the incident beam of electrons eject the orbital electrons of the atom by leaving holes in the shell and the electrons from an outer most shell with higher-energy then drop and fill these holes. The difference in energy between the levels results in the form of X-rays and it is measured by an energy-dispersive spectrometer. Thus, the elemental composition of the sample was determined from the position of the peaks in the spectrum.

The spectrum of our sample, shown in figure 2, is obtained in the energy range between 0 and 5 keV by using Quanta 400 F scanning electron microscope together with EDXA spectrometer.

The ratio of elements Ag:In:S in the sample was determined to be 6.76:36.37:56.86, respectively.

### 3.2 Spectral distribution of PC

The PC spectrum of the sample at different light intensities at a constant temperature of 80 K is illustrated in figure 3. As it is common in other semiconductors, i.e., ZnS, CdS, CdSe, Si, GaAs, PbS and InSb, each spectrum of our  $\text{AgIn}_5\text{S}_8$  sample also consists of a single peak at  $1.88 \pm 0.01$  eV ( $659 \pm 3$  nm). The PC is always much larger than that of the dark current at low temperatures. The absorption constant of  $\text{AgIn}_5\text{S}_8$  crystal [1] rapidly rises to  $\sim 2 \times 10^4$   $\text{cm}^{-1}$  at photon energies larger than 1.9 eV, at which the PC is controlled by high surface recombination rate near the surface of the sample causing the low PC. The number of photoexcited carriers

increased by the increase in light intensity, which causes the increases with the PC. However, both the shape and the position of the peak remain constant at different light intensities. From figure 3 it may also be noticed that the slope at low energy side of PC peak is quite sharp compared to that at higher energy side.

The spectral distributions of PC at different constant temperatures are shown in figure 4. The steep decrease in the intensities of the PC with the increase of temperature are attributed to the thermal quenching process. However, thermal quenching is more apparent in the PC spectra recorded, while temperature is rising at constant rates, the mechanism is discussed thoroughly in section 3.3. Furthermore, figure 4 reveals that the position of the maximum of the PC moves to lower energies with the increase in temperature.

The energy bandgap of the sample at various temperatures are determined by the use of Moss rule [21]. The wavelength dependence of the photosensitivity of the sample  $S(E)$  is defined as the ratio of photoconductivity  $\sigma(E)$  to its maximum value  $\sigma_{\text{max}}$  by the Moss rule as

$$S(E) = \frac{\sigma(E)}{\sigma_{\text{max}}} = \frac{1}{1 + \exp[C(E_g - E)]}, \quad (3.2.1)$$

where  $C$  is a constant and  $E_g$  the bandgap. The  $E_g$  is determined from the data for the first half of the peak in the PC spectrum.

Figure 5 shows the estimated energy bandgap of the sample at various temperatures by the use of Moss rule. The decrease in the band gap energy of  $\text{AgIn}_5\text{S}_8$  crystal with increase in temperature as in other crystals is clearly seen in figure 5. Unfortunately, only a limited number of data points could be obtained in a narrow temperature range between 80 and 140 K, because the intensity of the PC sharply decreases

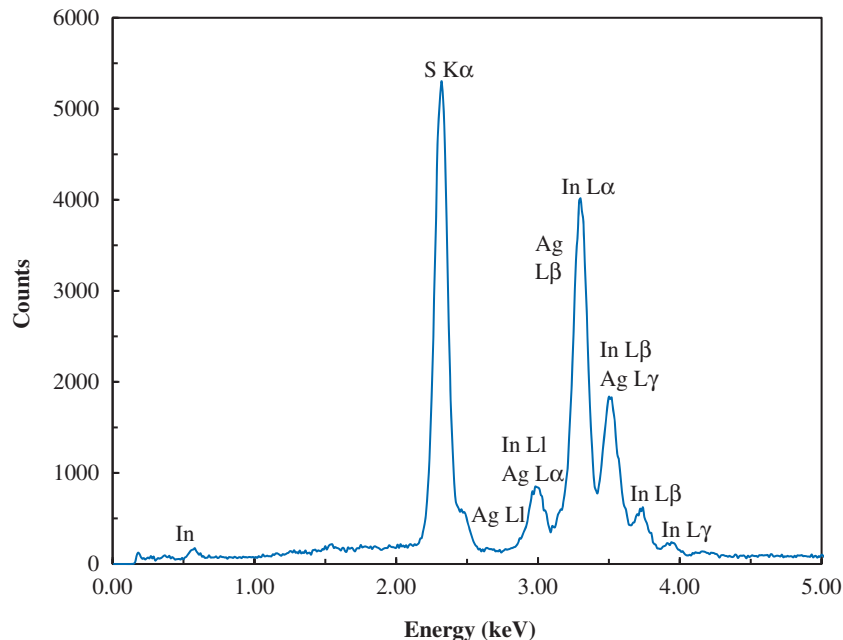


**Figure 2.** The EDXA spectrum of  $\text{AgIn}_5\text{S}_8$  sample.

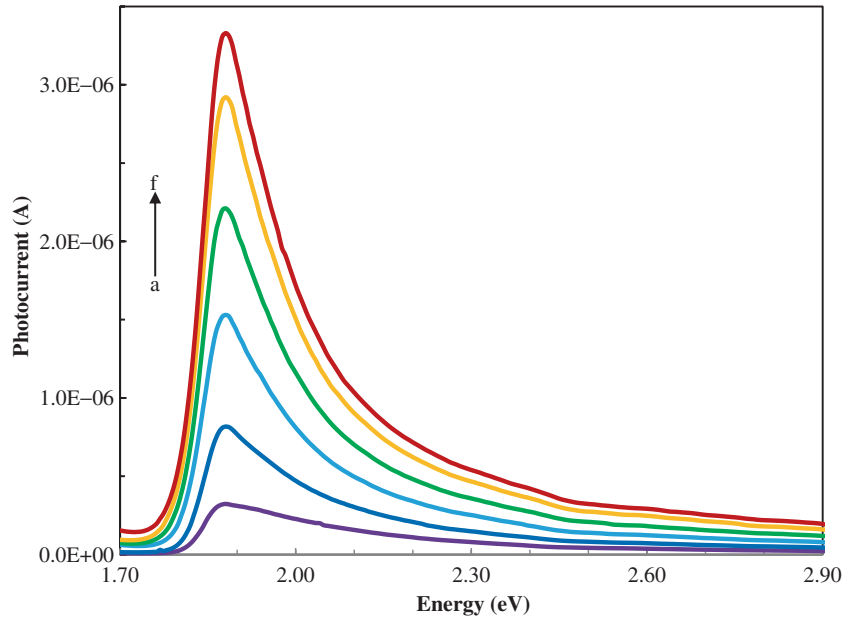


**Figure 3.** PC spectrum of the sample at various light intensities at 80 K: (a)  $1.0 \times 10^{13}$ , (b)  $2.0 \times 10^{13}$ , (c)  $4.0 \times 10^{13}$ , (d)  $8.0 \times 10^{13}$ , (e)  $1.6 \times 10^{14}$  and (f)  $3.2 \times 10^{14}$  photons  $\text{cm}^{-2} \text{s}^{-1}$ .

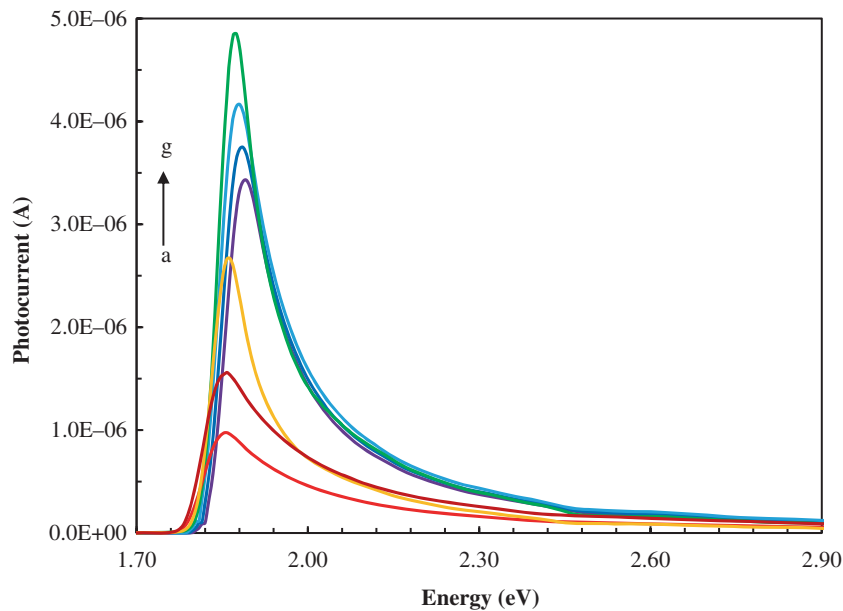


**Figure 4.** PC spectrum of the sample at  $3.2 \times 10^{14}$  photons  $\text{cm}^{-2} \text{s}^{-1}$  at various temperatures: (a) 140, (b) 130, (c) 120, (d) 80, (e) 90, (f) 100 and (g) 110 K.

due to the thermal quenching of the PC at such low temperature and then the peak becomes very broad for higher temperatures not to allow precise determinations.

The temperature dependence of the bandgap energy of the sample is given as [22]:

$$E_g(T) = E_g(0) - aT^2/(T + b), \quad (3.2.2)$$

where  $a$ ,  $b$  and  $E_g(0)$  are the temperature coefficient of the energy gap, the Debye temperature and the bandgap energy

at 0 K, respectively. When the data for our  $\text{AgIn}_5\text{S}_8$  sample from figure 5 is best fitted to the formula above in Equation (3.2.2),  $E_g(0)$ ,  $a$  and  $b$  are found to be 1.88 eV,  $1.1 \times 10^{-3} \text{ eV K}^{-1}$  and 200.0 K, respectively. It may be due to different crystal growing conditions of  $\text{AgIn}_5\text{S}_8$  crystal that the published data for these quantities are scattered from one to another. The bandgap value is found as low as 1.76 eV [23]. However, our bandgap value of 1.86 eV agrees well within the experimental error with 1.88 eV at 77 K [4].

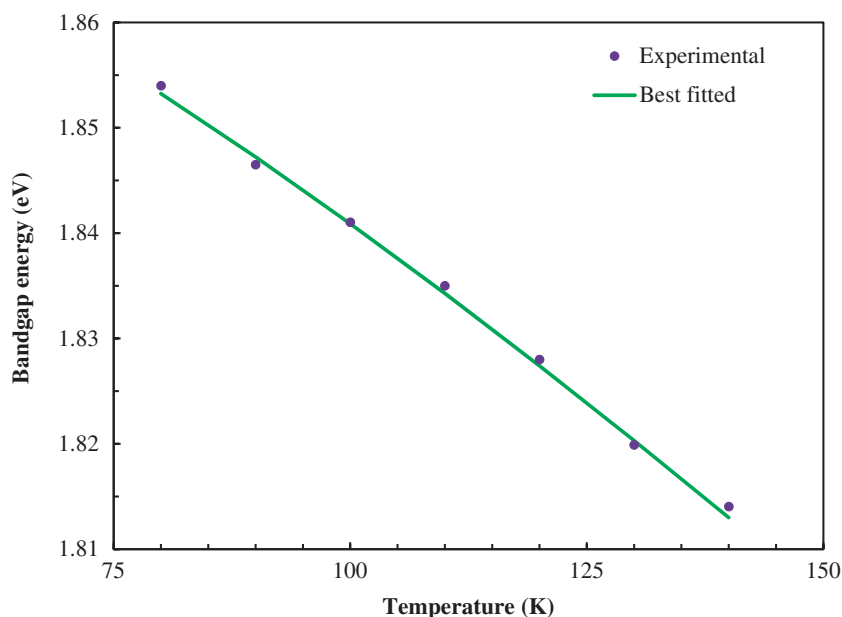


**Figure 5.** The variation of bandgap energy as a function of temperature.

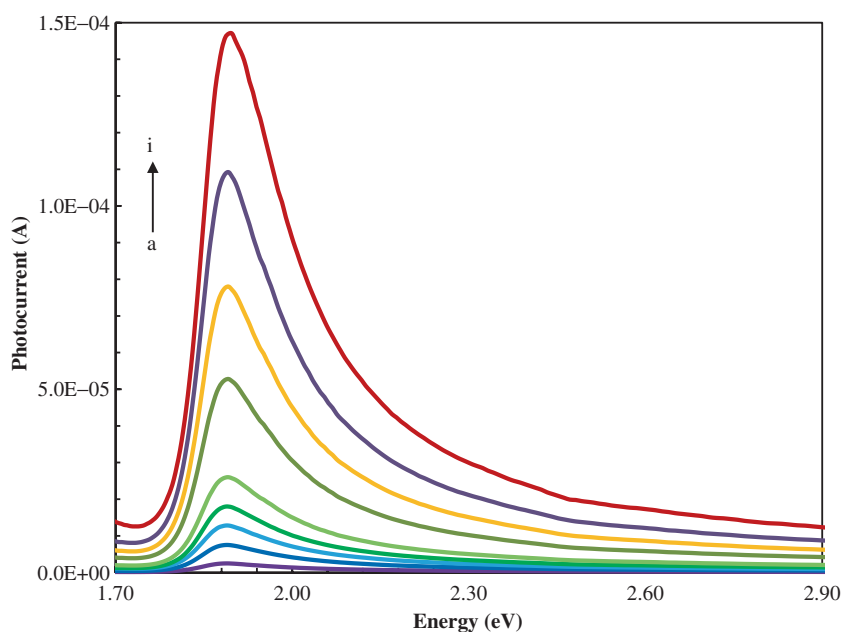


**Figure 6.** PC at 80 K at different bias voltages for light intensity of  $3.2 \times 10^{14}$  photons  $\text{cm}^{-2} \text{s}^{-1}$ : a-i are for applied voltages of 0.1, 0.3, 0.5, 0.7, 1.0, 2, 3.0, 4.0 and 5.0 V, respectively.

The Debye temperature of 250 K from Lindemann's melting method is considered to agree with our calculation [6]; however, there are some discrepancies in the temperature coefficients between our results and the previously reported ones as  $3.2 \times 10^{-4}$  and  $4.9 \times 10^{-4} \text{ eV K}^{-1}$  [12].

In addition, the PC spectra of  $\text{AgIn}_5\text{S}_8$  sample at various voltages for constant light intensity of  $3 \times 10^{14}$  photons  $\text{cm}^{-2} \text{s}^{-1}$  are measured and it is found that the position of the peak in the spectrum does not change but the intensity of the PC increases with increase in voltages (figure 6). The height

of the PC peak is found to rise linearly with the voltage in the range between 0.1 and 5.0 V. This result simply reveals that the mobility of the photogenerated carriers is independent of the electric field in the range of applied voltage under constant intensity of light. Similarly, the dark current as a function of bias voltage at various constant temperatures between 80 and 230 K is measured. Each curve consists of a single region dominating an ohmic behaviour and no space charge limited region is apparent up to 20 V. It means that, the number of thermally generated charge carriers in the volume of

the sample is very much larger than the number of injected carriers in the range of applied voltage.

In the present work, one of the major interest is to investigate the effect of the charge traps on the PC characteristics of  $\text{AgIn}_5\text{S}_8$  sample. Therefore, the effects of successive measurements and the pre-illumination on the PC spectra are studied. Figure 7 shows the PC spectra of the sample for seven successive measurements at 80 K. The intensity of the

PC increases with the increase of successive measurement and then it eventually reaches saturation.

Similarly, figure 8 also shows some increases in the PC due to pre-illumination at wavelength of 659 nm at temperature 80 K.

The figure shows that the enhancement in PC lasts long until the traps become empty. This indicates that the effect is reversible and the initial state is found to be established after heat-treating the crystal in the dark at  $\sim 180$  K. However,

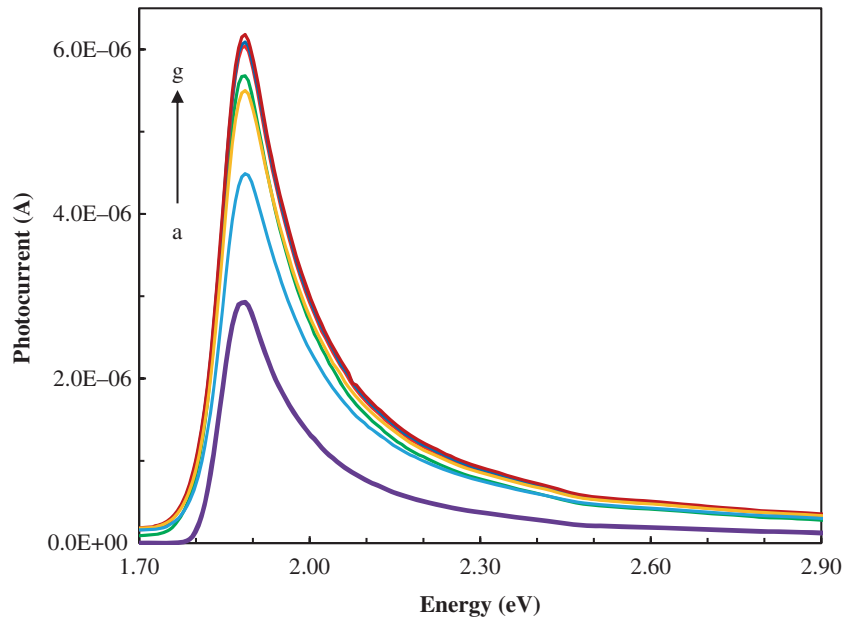


**Figure 7.** Successive PC spectra (a–g) with light intensity of  $3.2 \times 10^{14}$  photons  $\text{cm}^{-2} \text{s}^{-1}$  at 80 K.

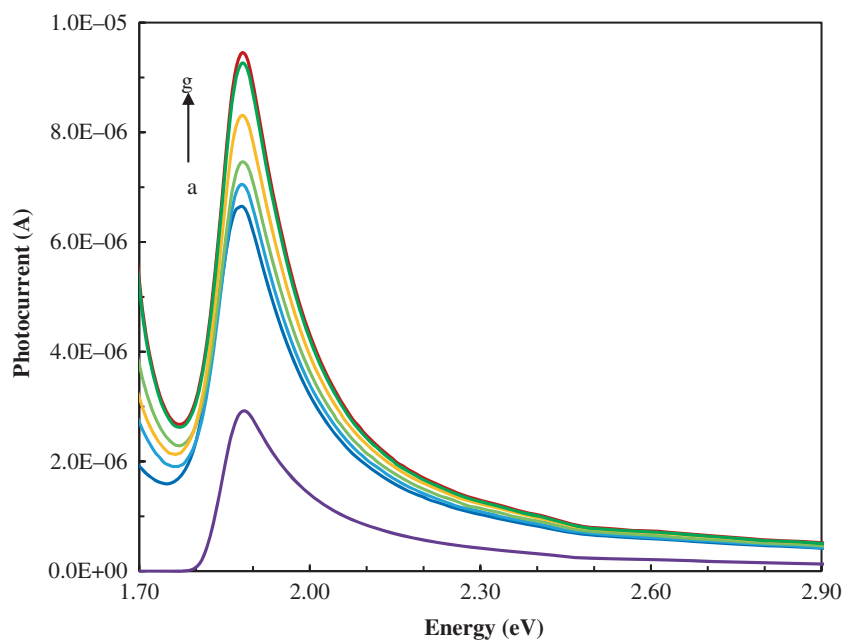


**Figure 8.** PC spectrum of the sample at 80 K: (a) without pre-illumination, (b–g) are after pre-illumination with light having photon energy 1.88 eV at intensities of  $3.0 \times 10^{14}$  photons  $\text{cm}^{-2} \text{s}^{-1}$  for 2, 4, 8, 15, 30 and 20 min, respectively.

in order to obtain the initial state we always heat the sample to room temperature.

### 3.3 Temperature dependence of PC

The PC at various light intensities at photon energy of 1.88 eV together with dark background current is shown in figure 9.

Both the structure of the spectrum and the PC peak temperature do not change, but the magnitude of PC increases with increase in the intensity of light. The whole PC spectrum consists of only a single broad peak at low temperature and then the current continuously rises up to higher temperatures as in the case of the dark current. Analysis of the curves in figure 9 shows that an increase is obtained in the PC as the

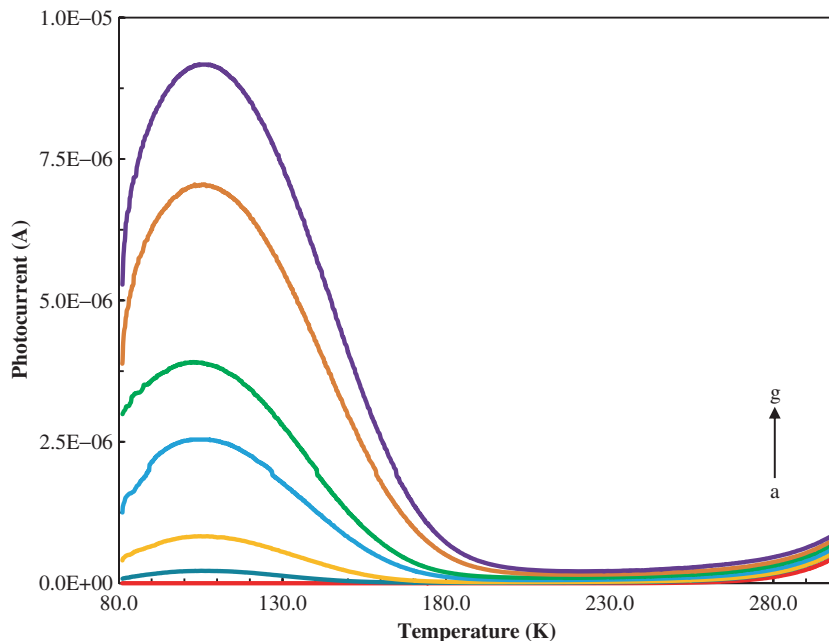


**Figure 9.** Temperature dependence of (a) dark current. (b–g) are the PCs at intensities of  $1.0 \times 10^{13}$ ,  $2.0 \times 10^{13}$ ,  $4.0 \times 10^{13}$ ,  $8.0 \times 10^{13}$ ,  $1.5 \times 10^{14}$  and  $3.0 \times 10^{14}$  photons  $\text{cm}^{-2} \text{s}^{-1}$  of light, respectively, at 659 nm.

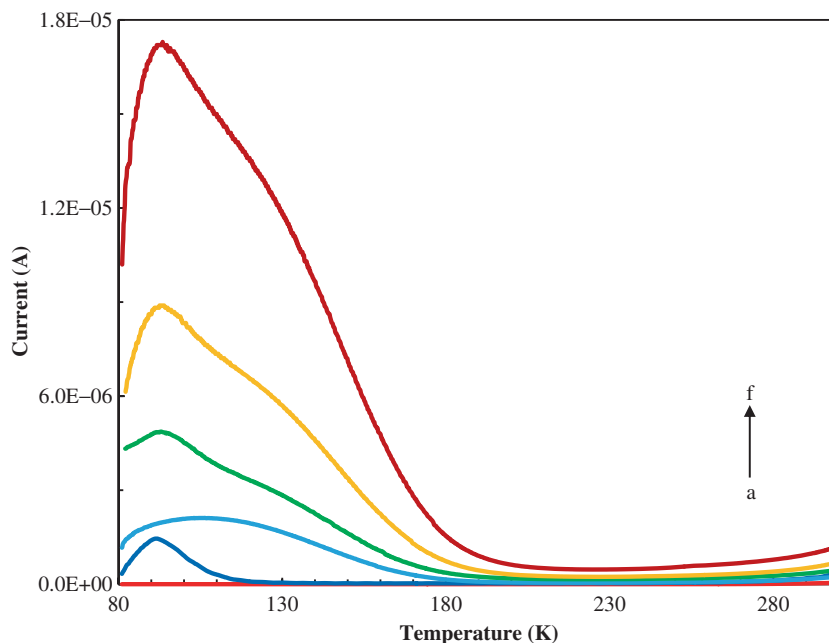


**Figure 10.** Temperature dependence of (a) dark background current, (b) TSC after illumination for 15 min with bandgap light having intensity of  $2 \times 10^{14}$  photons  $\text{cm}^{-2} \text{s}^{-1}$ , (c) PC without pre-illumination, (d–f) are the PCs at intensity of  $3 \times 10^{14}$  photons  $\text{cm}^{-2} \text{s}^{-1}$  after pre-illuminations for 4, 8 and 16 min, respectively, at 80 K.

temperature rises up to  $\sim 105$  K, due to both the electron and the hole quasi Fermi levels move apart from the band edges with the increase in temperature. That is, while the temperature rises, the Fermi level passes the hole recombination centre, which causes to decrease the probability of capturing electrons, thus the increased lifetime of electrons causes the rise in PC. In addition, during the PC measurement, the traps at low temperature start to be filled and a number of mobile carriers are then thermally released from the traps while the temperature is rising. However, the PC starts to decrease with increase in temperature above  $\sim 105$  K, which is considered to be due to both consequence of exhaustion of the initially filled traps and the well-known process called as thermal quenching of the PC. The thermal quenching process is explained by the 'two-centre model' developed by Bube [17]. According to the model, the crystal has two recombination centres. The main recombination centres have relatively large values of capture cross-sections for both type of charge carriers. The second recombination centres capture holes readily, but they have a low probability of capturing electrons. The energy at which the carriers have an equal probability of being thermally reemitted to continuous bands, or being captured by a deep recombination centre, is called the demarcation level. The demarcation levels [24] for holes and electrons locate close to the continuous bands at low temperatures under constant intensity of light. When the demarcation level associated with the second centres lies below these levels, photosensitivity increases due to increase in lifetime of the electrons. In other words, some of the created holes are now in the second centres so that the produced electrons in the conduction band cannot find enough number of holes to recombine in the first centres, and hence the lifetime of electrons, thus the photosensitivity increases. When the same demarcation levels move from below to above the second level with increase in temperature, lifetime of electrons is shortened resulting in the quenching of the PC (figure 9).

The trap filling dynamics is directly observed in the PC spectrum after pre-illumination of the sample. The PC spectra after various periods of time of pre-illumination and the correlation between the TSC and the PC is shown in figure 10. The contribution of TSC to PC appears clearly as a peak at  $\sim 90$  K in the spectra after pre-illumination. In addition, the same figure shows that a high degree of filling of the traps causes a marked enhancement in the intensity of the PC. By heating the sample for  $\sim 180$  K, the traps are emptied by thermal emission and the initial state is established. However, as stated before, a complete restoration is achieved by heating the sample up to room temperature. Because of the continuous illumination while heating, the filling of the traps must have the major contribution in the increase of the PC at early temperatures. These results clearly imply that the intensity of the PC are governed by the trapping process. We interpreted the temperature-dependent PC by considering two different contributions. The first is due the photoexcitation of the carriers and the second is due to the charges released from the traps filled during irradiation. Because of the continuous illumination during PC measurement, the traps are

filled first and then they are emptied in turns while the temperature is rising. All traps in the sample are found to be occupied by the charge carriers by irradiation at 80 K for 20 min with the light having a photon energy 1.88 eV at an intensity of  $3.0 \times 10^{14}$  photons  $\text{cm}^{-2} \text{s}^{-1}$ . The increase in the PC due to both successive measurements (figure 7) and pre-illuminations (figure 8) are directly associated with the occupancy of the traps in the sample. The magnitude of PC is correlated to the charge carrier concentration of the traps and we simply explain the enhancement of the photoconductivity due to pre-illumination or successive run as follows: the increases in PC are due to the increased lifetime of the photogenerated free carriers when the traps are filled. The mechanism for the increase in the lifetime of the photogenerated carriers due to occupancy of trapping centres is explained by considering the competition between recombination and the trapping centres [25]. The probability of trapping is high if the traps are not occupied, the lifetime will be short due to trapping being dominant. When the traps are occupied, the lifetime of the photogenerated carriers is high due to the dominance of the recombination process. In literature, the PC properties of various materials, for instance semi-insulating GaAs [26,27] and CdS crystals [17], are published to be strongly affected by illumination history. This effect is explained by some models [17,26–28], which are based on the reversible process in which the new complex defects are created and destructed in the bandgap of samples. However, both TSC and the temperature-dependent PC behaviour of our  $\text{AgIn}_5\text{S}_8$  sample do not indicate any possibility of creation of new defects after enhanced sensitivity to light.

#### 4. Conclusion

$\text{AgIn}_5\text{S}_8$  crystal studied in this work exhibits a PC at least four orders of magnitude higher than the dark current for even low ( $1 \times 10^{13}$  photons  $\text{cm}^{-2} \text{s}^{-1}$ ) intensity of light at low temperature. The temperature dependence of the PC spectra reveals a maximum at a low temperature and the position of the maximum remains constant as the intensity of illumination is increased. The PC spectra remain constant with the change in both light intensity and bias voltage. Thermal quenching of the PC is observed to begin at  $\sim 105$  K and it is completed at  $\sim 180$  K. The sensitivity to light of  $\text{AgIn}_5\text{S}_8$  sample is observed to be directly proportional to the degree of occupancy of the traps. A great enhancement of the PC is found due to pre-illumination of the sample with light having photon energy of 1.88 eV and maximum performance with  $\text{AgIn}_5\text{S}_8$  sample is achieved after filling all traps. Further study is certainly required to know how the photoelectric properties are affected by the density and the distribution of the traps in the bandgap of  $\text{AgIn}_5\text{S}_8$  crystal when intentionally doped and/or grown under different conditions. In addition, it may be a valuable separate future work to study the effect of oxygen on the photosensitivity and trap distribution of  $\text{AgIn}_5\text{S}_8$  crystals.

## References

- [1] Usujima A, Takeuchi S, Endo S and Irie T 1981 *Jpn. J. Appl. Phys.* **20** L505
- [2] Qasrawi A F, Kayed T S and Ercan I 2004 *Mater. Sci. Eng. B-Adv.* **113** 73
- [3] Delgado G E and Mora A J 2009 *Chalcogenide Lett.* **6** 635
- [4] Orlova N S, Bodnar I V and Kudritskaya E A 1998 *Cryst. Res. Technol.* **33** 37
- [5] Paorici C, Zanotti L, Romeo N, Sberveglieri G and Tarricone L 1977 *Mat. Res. Bull.* **12** 1207
- [6] Qasrawi A F and Gasanly N M 2001 *Cryst. Res. Tech.* **36** 457
- [7] Lee S J, Kim J E and Park H Y 2003 *Jpn. J. Appl. Phys.* **42** 3337
- [8] Lin L H, Wu C C and Lee T C 2007 *Cryst. Growth Des.* **7** 2725
- [9] Sinha M M, Ashdhir P, Gupta H C and Tripathi P P 1995 *Phys. Status Solidi B* **187** K33
- [10] Yao P, Wei D, Zhao X, Kang S Z, Li X and Mu J 2011 *Adv. Mat. Res.* **239–242** 3302
- [11] Damaskin I A, Pyshkin S I, Radautsan S I and Tezlevan V E 1973 *J. Exp. Theor. Phys. Lett.* **18** 239
- [12] Gasanly N M, Serpenguzel A, Aydinli A, Gurlu O and Yilmaz I 1999 *J. Appl. Phys.* **85** 3198
- [13] Cheng K W and Wang S C 2009 *Sol. Energ. Mat. Sol. C* **93** 307
- [14] Bodnar I V, Kudritskaya E A, Polushina I K, Rud V Yu and Rud Yu V 1998 *Semiconductors* **32** 933
- [15] Bodnar I V, Gremenok V F, Rud V Yu and Rud Yu V 1999 *Semiconductors* **33** 740
- [16] Lai C H, Chiang C Y, Lin P C, Yang K Y, Hua C C and Lee T C 2013 *ACS Appl. Mater. Interfaces* **5** 3530
- [17] Bube R H 1960 *Photoconductivity of solids* (New York: John Wiley & Sons Inc.)
- [18] Woods J 1958 *J. Electronics Control* **5** 417
- [19] Kononov I, Makhova L and Roussak L 2009 *Phys. Status Solidi A* **206** 1067
- [20] Ozdemir S, Bucurgat M and Firat T 2014 *J. Alloy Compd.* **611** 7
- [21] Moss T S 1952 *Photoconductivity in the elements* (London: Butterworths)
- [22] Varshni Y P 1967 *Physica (Utrecht)* **34** 149
- [23] Bodnar I V, Karoza A G, Korzun B V and Smirnova G F 1981 *Inorg. Mater.* **17** 152
- [24] Rose A 1978 *Concepts in photoconductivity and allied problems* (New York: Krieger Publishing)
- [25] Bube R H 1992 *Photoelectronic properties of semiconductors* 1st edn (Cambridge: Cambridge University Press)
- [26] Jimenez J, Hernandez P, de Saja J A and Bonnafé J 1987 *Phys. Rev. B* **35** 3832
- [27] Jimenez J, Gonzales M A, Hernandez P, de Saja J A and Bonnafé J 1985 *J. Appl. Phys.* **57** 1152
- [28] Stulen R H and Ascarelli G 1977 *Phys. Rev. B* **15** 1161